Journal of Alloys and Compounds 565 (2013) 127–133

Contents lists available at SciVerse ScienceDirect

Journal of Alloys and Compounds

journal homepage: www.elsevier.com/locate/jalcom

Mechanical properties of Cr-alloyed $MoSi_2$-based nanocomposite coatings with a hierarchical structure

Jiang Xu [a,*], Jia di Wu [a], Zhengyang Li [b], Paul Munroe [c], Zong-Han Xie [d]

[a] Department of Material Science and Engineering, Nanjing University of Aeronautics and Astronautics, 29 Yudao Street, Nanjing 210016, PR China
[b] Institute of Mechanics, Chinese Academy of Sciences, Beijing 100190, PR China
[c] School of Materials Science and Engineering, University of New South Wales, Sydney, NSW 2052, Australia
[d] School of Mechanical Engineering, University of Adelaide, SA 5005, Australia

ARTICLE INFO

Article history:
Received 29 October 2012
Received in revised form 19 February 2013
Accepted 20 February 2013
Available online 6 March 2013

Keywords:
Transition metal silicides
First-principle calculation
Nanocomposite
Mechanical properties
Residual stresses

ABSTRACT

Novel Cr-alloyed $MoSi_2$-based nanocomposite coatings were successfully synthesized onto Ti–6Al–4V substrates by a double glow discharge plasma technique. The architecture of the nanocomposite coatings exhibited a hierarchical structure, consisting of equiaxed C40-$MoSi_2$ with a bimodal grain size distribution and strip-shaped Mo_5Si_3 grains segregated to the boundaries of submicron $MoSi_2$ grains. The results showed that the toughness of the $MoSi_2$-based nanocomposite coatings depended strongly upon their hierarchical structure and the magnitude of compressive residual stresses in the nanocomposite coatings.

1. Introduction

Owing to its unique combination of a high melting point, superior high-temperature stability and strength, and excellent oxidation resistance at high temperatures, molybdenum disilicide ($MoSi_2$) has received much attention as a promising coating material for structural application in extremely harsh environments [1]. However, monolithic $MoSi_2$ suffers some severe deficiencies, such as poor low ambient temperature toughness and pest oxidation at moderate temperatures, which restrict its application as a protective coating [2,3]. Much effort has been devoted to overcoming these problems through substitutional alloying or forming nanocomposites [4–6]. For example, Cr additions can mitigate pest oxidation of $MoSi_2$ due to Cr having a strong affinity to oxygen [7,8]. $MoSi_2$ is a dimorph compound, which possess a hexagonal close-packed C40 structure with a $P6_222$ space group between the melting point and 1900 °C and a tetragonal body-centered $C11_b$ structure with a I4/mmm space group below this temperature [9,10]. In comparison with the well investigated $C11_b$ structured $MoSi_2$, little work has addressed the issue of the mechanical behavior of C40 structured $MoSi_2$, which is mainly attributed to the difficulty in fabricating metastable C40-structured $MoSi_2$ through conventional processing methods. Theoretical calculations have revealed that the reduction of symmetry from $C11_b$ structured to C40 structured $MoSi_2$ can lead to an improvement in ductility [11]. Therefore, it is imperative to explore different strategies to toughen monolithic C40 structured $MoSi_2$.

In this study, the influence of Cr additions on the lattice constants and mechanical parameters (bulk modulus, shear modulus, Young's modulus, and Poisson's ratio) of C40 structured $MoSi_2$ were explored by first-principles calculations based on density functional theory. Furthermore, $MoSi_2$-based nanocomposite coatings with varying Cr contents were deposited on Ti–6Al–4V substrates by a double glow discharge plasma technique. The effects of microstructural feature, Cr contents and compressive residual stresses on the mechanical properties of $MoSi_2$-based nanocomposite coatings were investigated.

2. Experimental method and computational details

Four Cr-alloyed $MoSi_2$-based nanocomposite coatings were deposited on mirror-polished Ti–6Al–4V alloy substrates by a double cathode glow discharge technique using four targets with different stoichiometric ratios ($Mo_{25}Si_{75}$, $Mo_{25}Cr_3Si_{72}$, $Mo_{23}Cr_5Si_{72}$ and $Mo_{20}Cr_8Si_{72}$), respectively. Inside the chamber, one cathode is used as the target and the other as the substrate, as described elsewhere [12]. The glow discharge sputtering conditions were as follows: base pressure, 4×10^{-4} Pa; target electrode bias voltage, −900 to −950 V; substrate bias voltage, −300 to −350 V; working pressure, 35 Pa; parallel distance between the source electrode and the substrate, 15 mm and treatment time of 3 h. The sputtering targets were fabricated from ball-milled Mo (99.99% purity), Cr (99.99% purity) and Si powders (99.99% purity) by employing cold compaction under a pressure of 600 MPa. Sub-

* Corresponding author.
E-mail address: xujiang73@nuaa.edu.cn (J. Xu).

0925-8388/$ - see front matter © 2013 Elsevier B.V. All rights reserved.
http://dx.doi.org/10.1016/j.jallcom.2013.02.134

strate materials used were Ti–6Al–4V alloy with a diameter of 40 mm and a thickness of 3 mm. Before sputter deposition, the substrates were polished using silicon carbide abrasive paper of 2400 grit and then ultrasonically cleaned in pure alcohol and water. For the sake of brevity, the coatings prepared using $Mo_{25}Si_{75}$, $Mo_{25}Cr_3Si_{72}$, $Mo_{23}Cr_5Si_{72}$ and $Mo_{20}Cr_8Si_{72}$ targets are referred to as M1(deposition temperature, 800 °C) and M2–4 (deposition temperature, 900 °C), respectively.

The phase compositions of the as-deposited coatings were studied using a X-ray diffractometer (XRD, D8ADVANCE with Cu Kα radiation) operating at 35 kV and 40 mA. X-ray data were collected using a 0.1° step scan with a counting time of 1 s. The as-deposited coatings were etched in Kroll's reagent (10 mL HNO_3, 4 mL HF and 86 mL distilled water) for 20–30 s. The microstructure and chemical composition of the as-deposited coatings were examined by scanning electron microscopy (SEM, Quanta 200, FEI Company) incorporating X-ray energy dispersive spectroscopy (EDS, EDAX Inc.) and transmission electron microscopy (TEM, Tecnai G220, FEI Company). Plan-view TEM samples were prepared using a single-jet electro-chemical polishing technique from the untreated side of the substrate. Nanoindentation tests were conducted on all the as-deposited coatings using a nanoindentation tester (an Ultra-Micro Indentation System (UMIS) 2000). Subsurface sectioning and imaging of indentation sites corresponding to a maximum load of 500 mN were carried out using a dual electron/focused ion beam (FIB) system (Nova Nanolab 200, FEI Company, Hillsboro, OR 97124, USA).

First-principles calculations were performed based on the plane-wave pseudopotential within the density functional theory (DFT) using the Cambridge Serial Total Energy Package (CASTEP) [13–15]. The interactions between ionic core and valence electrons were defined by the ultrasoft pseudo-potentials and the valence electrons considered for Mo, Cr and Si, were $4s^24p^64d^55s^1$, $3s^23p^63d^54s^1$ and $3s^23p^2$, respectively. The exchange–correlation energy was described by the generalized gradient approximation (GGA) with the Perdew–Burke–Ernzerhoh (PBE) [16] functional. Brillouin zone sampling was carried out using a $6 \times 6 \times 4$ set of Monkhorst–Pack *k*-points mesh and a plane-wave cutoff energy of 350 eV was employed in the calculations [17].

To generate compositions close to experimental stoichiometries, $2 \times 2 \times 1$ supercells consisting of 36 atoms were constructed for C40-structured $(Mo_{1-x}Cr_x)Si_2$ where Mo atoms were replaced by 1–3 Cr atoms and the corresponding Cr concentrations (i.e., '*x*' value) were 0.083, 0.167 and 0.250, respectively. Geometry optimizations were first performed to obtain equilibrium structures using Broyden–Fletcher–Goldfarb–Shanno minimization (BFGS) methods [18]. Both lattice parameters and atomic coordinates were relaxed until the total energy tolerance was smaller than 5.0×10^{-6} eV/atom, the maximum ionic Hellmann–Feynman force within 0.01 eV/Å, the maximum ionic displacement within 5.0×10^{-4} Å, and the maximum stress within 0.02 GPa.

3. Results and discussion

The mechanical parameters for C40-structured $(Mo_{1-x}Cr_x)Si_2$, including bulk modulus (*B*), shear modulus (*G*), Young's modulus (*E*), G/B ratio and Poisson's ratio (*v*), can be extracted from the calculated elastic constants by the Voigt–Reuss–Hill (VRH) approach [19]. The calculated mechanical parameters for C40-structured $(Mo_{1-x}Cr_x)Si_2$ are plotted in Fig. 1. Our calculated values for bulk modulus and shear modulus for binary C40 $MoSi_2$ differ from the theoretical values obtained by other investigations by only 3% and 1.6%, respectively, demonstrating the reliability of our present calculations [11]. As shown in Fig. 1a, with increasing Cr concentration, the bulk modulus, shear modulus and Young's modulus slightly increase. These quantities are of fundamental importance for understanding the mechanical behavior of materials. Since hardness depends mainly on plastic deformation associated with the creation and motion of dislocations, shear modulus exhibits a linear correlation with the hardness of materials [20,21]. As a result, Cr alloying may increase the hardness of C40-structured $MoSi_2$, resulting in solid solution hardening. Moreover, brittleness or ductility of a material is closely related to the elastic properties of a crystal. For instance, Pugh [22] proposed the ratio of bulk to shear modulus G/B, as a key parameter to distinguish brittle and ductile behaviors for a solid at a critical value of 0.57, where below this value the material behaves in a ductile manner; otherwise, the material behaves in a brittle manner. As shown in Fig. 1b, it is clear that C40-structured $(Mo_{1-x}Cr_x)Si_2$ can be classified as a brittle material based on the Pugh criteria, and the calculated G/B values for C40-structured $(Mo_{1-x}Cr_x)Si_2$ are essentially independent of Cr content. Poisson's ratio, *v*, provides more information about the characteristics of the bonding forces compared with other elastic constants [23]. It is generally assumed that the smaller Poisson's ratio, the stronger the directionality of atomic bonding. Our calculated values for Poisson's ratio are larger than that reported for $C11_b$-structured $MoSi_2$ and C40-structured $CrSi_2$, denoting that the directionality in atomic bonding in C40-structured $(Mo_{1-x}Cr_x)Si_2$ is weaker [24]. On the other hand, Poisson's ratio, characterizes the stability of the crystal against shearing strain, and is widely used as a useful criterion for brittleness [25]. Obviously, the variation of the Poisson's ratios for C40-structured $(Mo_{1-x}Cr_x)Si_2$ with Cr additions is similar to that for the G/B ratio.

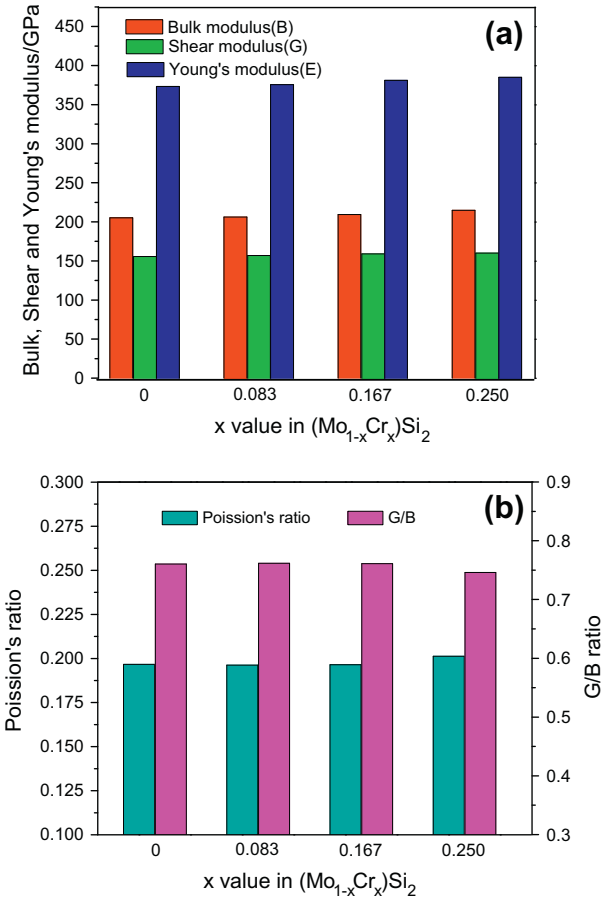

Fig. 1. The Calculated mechanical parameters for C40 structured $(Mo_{1-x}Cr_x)Si_2$: (a) Bulk, shear and Young's modulus; (b) Poisson's ratio and G/B ratio.

As shown in Fig. 2a, X-ray diffraction data reveal that the M1 coating consists of monolithic C40-structured $MoSi_2$ with a pronounced (1 1 1) orientation texture, whereas the M2–4 coatings are composed mostly of C40-structured $MoSi_2$ with minor concentrations of D8m-structured Mo_5Si_3. It should be noted, however, that C40-$MoSi_2$ can form as a metastable intermediate phase either during the phase transformation from amorphous to $C11_b$-$MoSi_2$ or during thin film deposition [26,27]. Similar to other PVD processes, the coatings grown by glow discharge deposition often exist in a non-equilibrium state, characterized by limited atomic assembly kinetics. Under such conditions, the mechanism of phase formation in the coatings is governed by the nucleation model, suggesting that the phase with either the fastest nucleation rate or the lowest nucleation barrier is the most likely to be formed. Because the activation energy for the formation of C40-$MoSi_2$ (1.5 eV) is smaller than that for $C11_b$-$MoSi_2$ (7.8 eV), the nucleation of the C40-$MoSi_2$ phase needs to overcome a lower energy barrier and, thus, can readily be formed during glow discharge deposition [27]. Moreover, the positions of $MoSi_2$ diffraction peaks for the four coatings shift to lower 2θ values with reference to the powder diffraction